Journal of Catalysis **188,** 203–214 (1999)
Article ID jcat.1999.2652, available online at http://www.idealibrary.com on IDEAL®

Oxidation of Toluene and *o*-Xylene on Ti Phosphate-Supported Vanadium Oxide Catalysts

S. del Val,* M. López Granados,* J. L. G. Fierro,*,[1] J. Santamaría-González,† and A. Jiménez-López†

*Instituto de Catálisis y Petroleoquímica (C.S.I.C.), Campus de la UAM, 28049 Madrid, Spain; and †Departamento de Química Inorgánica, Cristalografía y Mineralogía, Facultad de Ciencias, Universidad de Málaga, 29071 Málaga, Spain

Received May 19, 1999; revised August 6, 1999; accepted August 9, 1999

The oxidation of toluene and *o*-xylene on α-Ti$(HPO_4)_2 \cdot H_2O$-supported vanadium oxide catalysts is reported. Vanadium is incorporated at different loadings by $VOCl_3$ grafting and by vanadyl oxalate wet impregnation. Their catalytic properties and the results of the physico-chemical characterisation (Laser Raman, XRD, SEM, N_2 adsorption, XPS, and thermal analysis) were compared with those of a conventional V_2O_5/TiO_2 catalyst (with an 8 V_2O_5 wt% loading). It is shown that toluene oxidation is as selective in Ti-phosphate-based catalysts as in the conventional system, whereas *o*-xylene oxidation is less selective: a much lower phthalic anhydride yield is obtained. Vanadium uptake on Ti phosphate reaches a limit value when the grafting method is used: V_2O_5 loadings higher than 5 wt% cannot be surpassed. A vanadium oxide–Ti phosphate support interaction exists at V loadings lower than 5 V_2O_5 wt% as suggested by the fact that the same $VOPO_4$-like environment is detected irrespective of the method used to incorporate V. Higher vanadium loadings by using wet impregnation result in the formation of larger V_2O_5 crystallites than in the case of the conventional V_2O_5/TiO_2 catalyst. The lack of interaction at high V loadings leaves the support uncovered. The poorly covered Ti phosphate surface exposing acid surface sites must account for the lower *o*-xylene oxidation to phthalic anhydride.

Key Words: **toluene; *o*-xylene; selective oxidation; vanadium oxide; titanium phosphate.**

INTRODUCTION

The partial oxidation of alkylaromatics such as *o*-xylene and toluene results in the formation of products such as phthalic anhydride, maleic anhydride, benzaldehyde, and benzoic acid. These products have higher added value because they are used in industrial processes for the synthesis of plastics, polyester resins, plasticizers, pesticides, dyes, etc. (1–4). Indeed, the oxidation of *o*-xylene is now well implemented in industry and has replaced the older process based on the oxidation of naphthalene to obtain phthalic anhydride (2). The best catalyst known so far for *o*-xylene and toluene oxidation is V_2O_5 supported on anatase, one of the isomorphs of TiO_2 (5–7). This system has been characterised in depth, and it has been reported that the P is present in industrial catalysts (2, 3). The bulk percentage of promoters is very low, but they are concentrated at the surface (8), where their local concentration is much higher. There is some controversy in the literature as to whether P should be considered an impurity, a promoter, or a poison to the V_2O_5/TiO_2 system. Van Hengstum *et al.* have reported that it is not easy to obtain a P-free TiO_2 and that P is present at low bulk concentrations. These authors also showed that the addition of P to V_2O_5/TiO_2 improves the catalytic oxidation of toluene and *o*-xylene on the V–Ti–O system. Unfortunately, their results were incomplete because the yields to all possible products were not followed; despite this, the improvement of catalyst performance obtained with the addition of P was clearer at higher conversion (9). Wachs *et al.* (10) reported that the incorporation order of P and V is very important in the preparation of V–Ti–P–O catalysts used for the oxidation of methanol. Actually, van Hengstum *et al.* (9) impregnated V in a second step on a support previously impregnated with P. By contrast, Anderson *et al.* prepared the catalyst by simultaneous wet impregnation of V and P (11); this resulted in a clear reduction in the performance of the catalyst.

The above controversy prompted us to study the behaviour of the V–Ti–P–O system in the catalytic oxidation of alkylaromatics, not only to test the catalytic properties of this system but also to gain information on the role of P in such reactions. The approach followed in this work consisted in using a hydrated titanium hydrogenphosphate, α-Ti$(HPO_4)_2 \cdot H_2O$ (α-TiP), as a support since the impregnation of TiO_2 by P results in the formation of Ti hydrogen phosphate (12). This solid has already received much attention (13–18), which is obviously an advantage as regards gaining insight into the role of P in the catalytic properties of the V–Ti–O system.

The actual method of adding vanadium to anatase has been reported not to affect the final chemical and catalytic properties of vanadium oxide. In this sense, chemical

[1] To whom correspondence should be addressed. Fax: 00-34-91-5854760. E-mail: jlgfierro@icp.csic.es.

0021-9517/99 $30.00

vapour deposition or grafting by vanadyl chloride or vanadium alkoxides (19, 20), incipient wetness impregnation or wet impregnation of any vanadium-containing salt (21), or solid state reactions between V_2O_5 and anatase when calcined or under reaction environment (22) all essentially result in the same V_2O_5/TiO_2 system as long as other variables, such as the percentage composition or temperature of calcination, are the same and as long as the system has reached the chemical equilibrium. V_2O_5 wets the TiO_2 surface via a strong interaction between the surface of TiO_2 and VO_x moieties (7, 22–25). Here, the effect of the method of vanadium deposition on the vanadium oxide–support interaction, and therefore on its catalytic properties, is studied. The first method, $VOCl_3$ grafting, is based on the ability of vanadium chloride to react with an acid –*X*–OH (*X* can be P or Ti), which affords a monolayer of vanadium oxide on the surface of the support. The second method, wet impregnation of vanadyl oxalate, is simple and safe, and it allows the deposition of higher vanadium oxide loadings. A comparison of both methods should provide information about the conditions, if any, under which the vanadium oxide–Ti phosphate support interaction develops and the effects it has on the properties of the catalyst.

EXPERIMENTAL

Preparation of Catalysts

The support was prepared by a sol–gel methodology. A solution of $Ti(OiPr)_4$ (Aldrich purity 93%) in *n*-propanol (Prolabo pure quality) was hydrolysed by slow addition of 1 M H_3PO_4 (final P/Ti = 1). The gel thus obtained was solubilised in 85% H_3PO_4 (Analar) (P/Ti = 10.2), and after 5 h of vigorous stirring at 295 K a white gel was formed. Stirring was then maintained for a further 70 h. The solid was rinsed in several cycles of centrifugation and addition of *n*-propanol and finally with distilled water, and it was finally air-dried at 333 K. This solid was called α-TiP, and its XRD pattern corresponded to $Ti(HPO_4)_2 \cdot H_2O$. The specific BET area of this uncalcined solid was 10 m^2/g.

The incorporation of vanadium to the support was accomplished following two different methods, grafting by $VOCl_3$ (Aldrich 99%) in organic medium and wet impregnation by vanadyl oxalate. The grafting procedure was carried out by stirring a suspension of the α-TiP solid in a solution of $VOCl_3$ in *n*-hexane at room temperature for 24 h. The α-TiP used for grafting was dried a 473 K and kept in dry atmosphere before $VOCl_3$ solution in *n*-hexane was added. The amount of $VOCl_3$ was varied in order to see whether it might be possible to increase the V loading. The atmosphere was carefully controlled in order to exclude humidity. The solid was rinsed with hexane. The wet impregnation technique was carried out using an impregnation solution prepared by adding V_2O_5 (Fluka >99% purity) to a solution of oxalic acid (Panreac 99.5%) in water (2.3 g oxalic acid/g V_2O_5) at 323 K. Addition must be slow enough to avoid loss of solution by spilling, due to the strong evolution of CO_2. The volume of the blue solution thus obtained was brought up to 30 cm^3, and then the support was added to the solution. Finally, the excess water was removed by evaporation in a rotary evaporator.

Precursors were air-dried at 333 K, and catalysts were obtained by calcining the precursors at 923 K in the case of grafted samples and at 723 K in the case of wet impregnated samples. The precursors are hereafter referred to as *x*VTiP*y*, where *x* indicates the expected wt% V_2O_5 of the samples according to the amount of V added during the preparation procedure and *y* denotes whether the sample was prepared by the grafting (g) or the impregnation (i) method. To indicate that the sample had been calcined (catalysts) the suffix "c" is added to the name of the precursor. Thus, 20VTiPi-c would be a catalyst obtained from a precursor prepared by the wet impregnation method with a theoretical 20 wt% V_2O_5.

A reference TiO_2 (anatase)-supported-V_2O_5 catalyst was prepared in order to compare some of the chemical and catalytic properties of the V–Ti–P–O system. The method used to add the V_2O_5 was the wet impregnation method explained above. The precursor was dried at 333 K and calcined at 723 K in dry air. Anatase was supplied by Than and Mulhouse (pigment grade). V_2O_5 loading was 8 wt%, and hence the precursor is referred to as 8VTi.

Characterisation of Samples

N_2 adsorption isotherms were recorded at the temperature of liquid N_2 with a Micromeritics ASAP 2000 apparatus. Samples were previously outgassed at 413 K for 6 h. XRD patterns were recorded on a Seifert 3000 diffractometer using Ni-filtered Cu$K\alpha$ radiation ($\lambda = 0.1541$ nm). Raman spectra were recorded on a single-monochromator Renishaw 1000 spectrophotometer equipped with a CCD cool detector (200 K), with an argon laser as the exciting source ($\lambda = 514.5$ nm), a single monochromator, a supernotch filter, and an *in situ* cell which enables treatment of samples under a flow of gases. Raman spectra were recorded at room temperature with a laser power of 2 mW. Chemical analysis of the samples to determine the V, Ti, and P composition was carried out by ICP using a Perkin–Elmer Optima 3300 DV apparatus. Samples were previously digested in a microwave oven using an $HF/HCl/HNO_3$ mixture. SEM micrographs were take with an ISI DS-130 microscope equipped with a secondary electron detector with a maximum resolution of 10 nm and with a Si(Li) Kevex detector, which allows chemical analysis by energy dispersion analysis of X-rays. Electrons can be accelerated in the 1–40 keV range. The sensitivity of the chemical analysis is 0.5% for elements $Z > 11$ in a minimum area of 1 μm^2.

Thermogravimetric analysis was carried out on a Perkin–Elmer TGA-7 apparatus. The samples (ca. 15 mg) were loaded and heated under a flow of dry air at a rate of 40 ml/min and a heating rate of 10 K/min. Thermal differential analysis was accomplished on Perkin-Elmer DTA-T equipment. The samples (ca. 40 mg) were heated under a flow of dry air at a rate of 100 ml/min and a heating rate of 10 K/min. Photoelectron spectra were acquired with a VG Escalab 200R spectrometer equipped with a hemispherical electron analyser and an Mg $K\alpha$ 120 W X-ray source. The powder samples were pressed into small aluminium cylinders and then mounted on a sample rod placed in an *in situ* pretreatment chamber and outgassed at room temperature for 1 h prior to being placed inside the analysis chamber. During data acquisition the pressure in the ion-pumped analysis chamber was maintained below 2×10^{-9} mbar. Intensities were estimated by calculating the integral of each peak after smoothing and subtraction of the "S-shaped" background and fitting the experimental curve to a combination of Lorentzian and Gaussian lines. All binding energies (BE) were referenced to the adventitious *C* 1*s* line at 284.9 eV. This reference gave BE values with an accuracy of ±0.2 eV.

Measurements of Catalytic Activity

Catalytic activity measurements were carried out in a plug-flow glass fixed-bed reactor heated by a cylindrical oven. Circa 0.06 g ($W/F = 42$ g s l^{-1}) of catalyst diluted seven times in carborundum was loaded (0.42–0.50 mm). Gas flows were controlled by mass flow controllers. Toluene (Fluka >99.8%) or *o*-xylene (Fluka >99%) were fed as liquid by means of a perfusion pump. Alkylaromatic and O_2 molar concentrations in the feed were 0.8 and 20.8%, respectively (balance N_2). The inlet lines were heated at 453 K in order to ensure the evaporation of alkylaromatics. A Varian gas chromatograph (Star 3400 CX) was connected on line with the reactor outlet in order to analyse permanent gases and volatile fractions of the reaction mixture. An ice bath trap was placed between the GC and the reactor outlet to condense part of the unreacted alkylaromatic and part of the products. The lines connecting the reactor and the trap were heated up to 523 K. The temperature of the bottom part of the reactor, downstream from the catalyst bed, was higher than 623 K. The GC was equipped with TCD and FID detectors. O_2, N_2, H_2O, CO, and CO_2 were separated by two packed columns connected in series (HayesSep D and 5 Å molecular sieve). Organic products were separated by an RTX-5 capillary column.

RESULTS

Table 1 summarises some of the physico-chemical properties of the catalysts. Fierro *et al*. have reported that 6VTiPg-c shows maximum V_2O_5 uptake when the grafting method is used (ca. 5 wt%) (26). Increasing the concentration of the grafting solution does not result in a stronger uptake of V. This value is defined by the availability of the reagent to surface OH groups. Some calculations can be done to estimate the amount of $VOCl_3$ able to react with surface OH groups. It must be considered that in the structure of $Ti(HPO_4)_2 \cdot H_2O$, each P–OH group occupies 0.2167 nm^2 (13) and when α-TiP support is calcined its specific area increases to 30.4 m^2/g. Assuming that (i) the density of phosphorous is kept after calcination of α-TiP and (ii) each P–OH group can anchor one $VOCl_3$ moiety, it can be concluded that only 2.2 V_2O_5 wt% can be anchored. It should be taken into account that Ti–OH groups can also react with vanadium chloride (in which case the value rises to 3.3 V_2O_5 wt%). It should be also considered that the surface was enriched in P (see XPS results below) and that Ti phosphate can be hydrolysed while vanadium is added, especially the surface, resulting in the breaking of the P–O–Ti bond and the forming of new Ti–OH and P–OH sites, which increases the amount of surface reactive groups (27). Thus, the saturation uptake of V by grafting must be greater than 3.3; experimentally it is ca. 4.7%.

TABLE 1

Physicochemical Properties of Catalysts

Catalyst	V_2O_5 wt% (theoretical)	V_2O_5 wt% (chem. anal.)	Number of monolayers[a]	BET surf. area (m^2/g)
α-TiP-c	0	0	0	30.4
1VTiPg-c	1	1.6	0.4	23.6
6VTiPg-c	6	4.7	1.1	23.9
2VTiPi-c	2	2.1	0.5	26.3
5VTiPi-c	5	4.3	1.0	19.7
10VTiPi-c	10	11.1	2.5	16.3
20VTiPi-c	20	20.5	4.7	11.0
8VTi-c	8	7.2	5.6	9.0

[a] Calculated assuming that V_2O_5 spreads over the surface of the precursor (30.4 m^2/g) and each V atom ($VO_{2.5}$) occupies 0.105 nm^2 of the support surface (40).

Obviously, a greater amount of V_2O_5 can be incorporated if the wet impregnation method is used. Regarding the BET specific surface area, the wet-impregnated series showed a decrease with the vanadium loading, readily explainable in terms of pore filling by the vanadium phase. Table 1 also summarises the theoretical number of monolayers of V_2O_5. This number was calculated assuming that V_2O_5 is formed after calcination and that it spreads over the surface, developing a "monolayer" of V_2O_5 (see Table 1). It should be stressed that since the Ti–P–O support has higher surface area than anatase after calcination, higher V loadings are required to obtain a similar theoretical dispersion of vanadium. In fact, the number of theoretical V monolayers of the 20VTiPi-c sample (20 wt%) was only slightly lower than that of the 8VTi-c sample (4.7 vs 5.6, respectively).

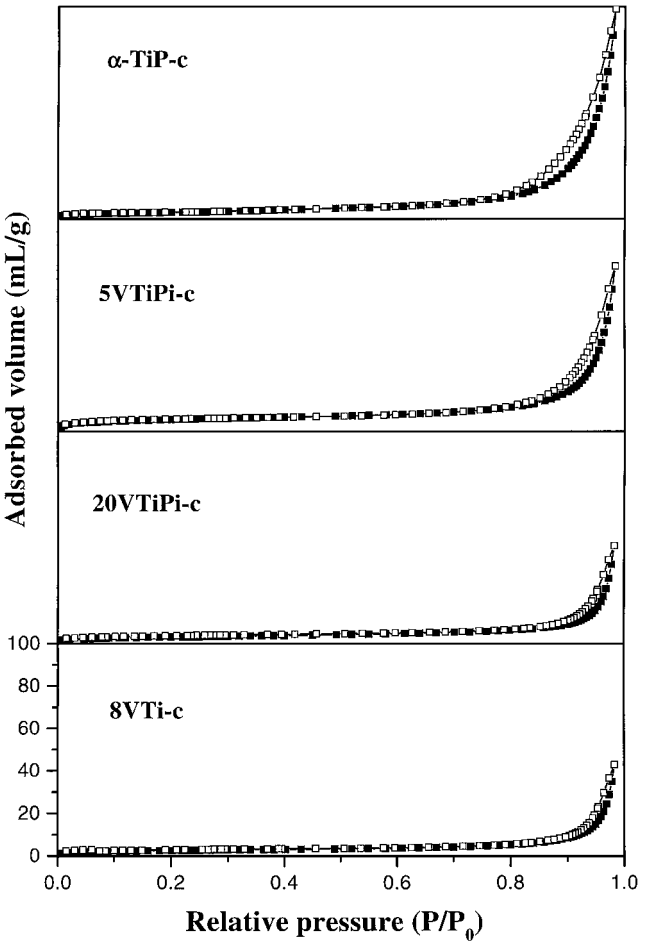

FIG. 1. N_2 adsorption and desorption isotherms of several catalysts, (closed symbols) adsorption branch, and (open symbols) desorption branch.

Figure 1 shows the N_2 isotherms of the calcined samples α-TiP-c, 5VTiPi-c, 20VTiPi-c, and 8VTi-c. The isotherms correspond to mesoporous materials of type A according to the de Boer classification (hysteresis type H3 according the IUPAC classification) (28). These types of isotherms and hysteresis loops are typical of mesoporous materials defined by plate-like particle aggregation. The figure clearly shows that the vanadium added to the support seems to fill the mesopores and therefore the space between the particles. Figure 2 offers SEM microphotographs of α-TiP-c and 20VTiPi-c. The V-free sample is shaped in plate-like particles clustered in a major extension in a rose-blossom-like shape. The 20VTiPi-c sample, the richest V catalyst, displays a similar morphology, and no grains of different morphology, suggesting phase segregation, were seen. Chemical analysis by EDAX revealed that this sample was homogeneous in all the spots analysed: V, Ti, and P were detected at molar concentrations closer to the composition determined by ICP. It can be concluded that at the resolution used to make the pictures no V phase segregation occurred.

Figure 3 shows the XRD patterns of some of the samples calcined at 723 K (however, as explained below, the diffractogram of the calcined precursor shown in the figure belongs to samples calcined at 1023 K instead of at 723 K). TGA and DTA analysis showed (see below) that at 723 K the transformation of hydrogenphosphate to layered pyrophosphate is not totally achieved and an ill-crystallised phase is reached. The rehydration of the remaining $Ti(HPO_4)_2$, the phase resulting from the partial dehydration of the support (the samples were stored under room air can occur. Indeed, the diffraction lines of the vanadium samples are broad and of low intensity, indicating that the samples are quite amorphous. The diffraction pattern with the clearest reflections belongs to the 20VTiPi-c sample. Peaks at 0.419, 0.341, 0.302, 0.290, and 0.250 nm together with the wide peak at around $2\Theta = 10^\circ$ suggest the presence of layered α-TiP_2O_7 (14). Evidence in favour of the notion that no cubic TiP_2O_7 peaks were present in the former diffractograms is that when the support is calcined at much higher temperatures (1023 K) than the V-containing samples (723 K) it displays the reflections of cubic-TiP_2O_7 ($d = 0.456$, 0.394, 0.353, 0.322, 0.279, 0.237, 0.218, 0.191, 0.176, 0.161, 0.152, and 0.139 nm) (29). (We show this diffractogram to demonstrate that crystalline cubic-TiP_2O_7 is absent in samples calcined at lower temperatures.)

One striking observation was that no diffraction lines arising from V_2O_5 or any other vanadium compound were detected. In order to verify the dispersion reached by the impregnation method, a physical mixture of the impregnating vanadium phase and support (20 wt% V_2O_5) was prepared as follows: the solid resulting from water evaporation of the impregnating vanadyl oxalate solution was mixed with the bare support and both were calcined together at 723 K. The XRD of this physical mixture is also shown in Fig. 3. Very intense V_2O_5 diffraction lines were visible. By contrast, such reflections are absent in the sample that has the same composition but was prepared by impregnation (20VTiPi-c). This result indicates that the V phases present either are amorphous or have a small crystal size, and then that the vanadium phase appears to be dispersed by the impregnation method.

The thermogravimetric analyses of several samples heated under a flow of air can be seen in Fig. 4a. The mathematically obtained differential curve is also plotted in order to clarify the weight loss processes (Fig. 4b). The TG traces for α-TiP, 6VTiPg, 5VTiPi, and 20VTiPi precursors are compared. The first loss of weight associated with hydration water, located between the layers of the phosphate, occurs in a wide temperature range, i.e., between room temperature and 573 K. This process affords the $Ti(HPO_4)_2$ (17, 18). The second weight loss corresponds to the evolution of water molecules existing in the structure, due to the condensation of HPO_4 groups, yielding

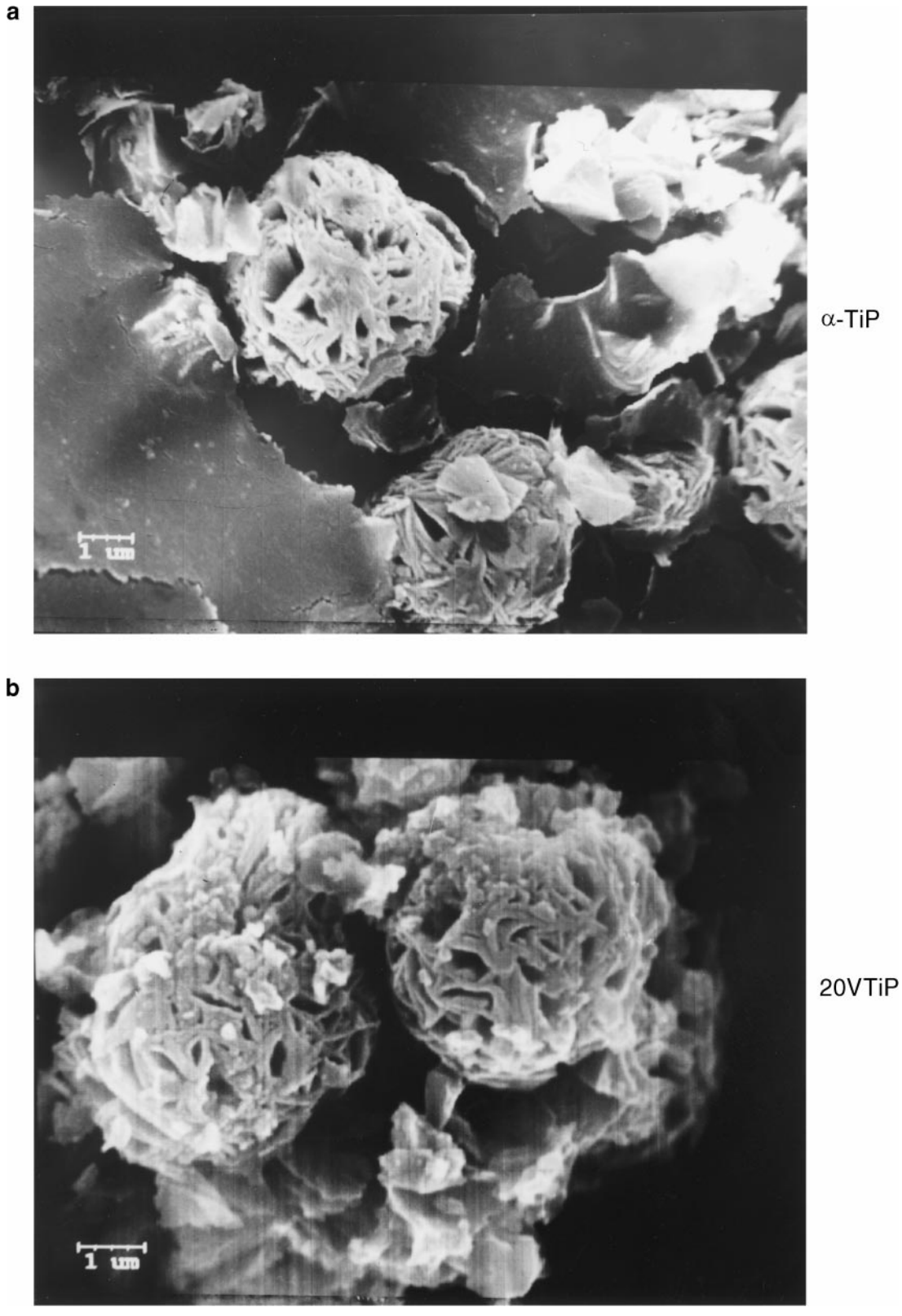

FIG. 2. SEM micrographs of (a) the α-TiP-c sample and (b) the 20VTiPi-c sample.

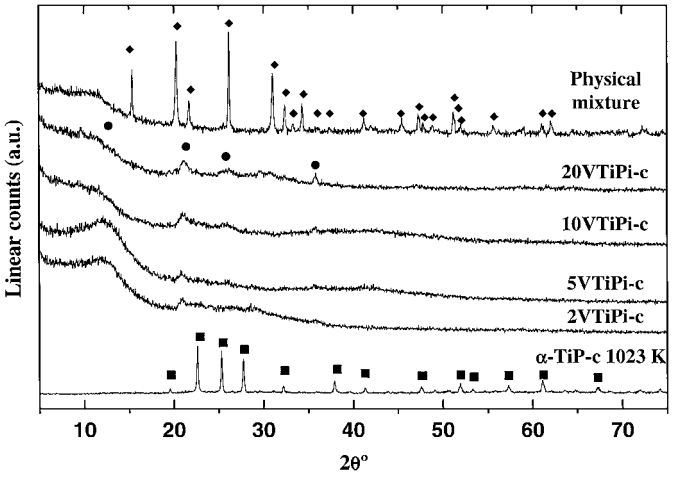

FIG. 3. XRD patterns of several catalysts. Vanadium-containing samples, including the physical mixture, were calcined at 723 K. The α-TiP-c diffractogram belongs to a sample calcined at 1023 K (◆, V_2O_5; ●, $Ti(HPO_4)_2 \cdot H_2O$; ■, cubic-TiP_2O_7).

the formation of layered Ti pyrophosphate (TiP_2O_7) (17, 18). In the vanadium-containing samples prepared by wet impregnation, together with these two processes, an additional loss of weight is also observed at ca. 523 K, which is superimposed on the first loss of water. This loss should be assigned to the removal of the oxalate residues introduced during wet impregnation. This feature, less visible in 5VTiPi, was clearly detected in the thermogravimetric analysis of 20VTiPi due to its higher oxalate loading and was not observed in the samples prepared by grafting.

Figure 5 shows the DTA curves obtained in the corresponding previous TGA experiments. The DTA pattern of α-TiP shown in Fig. 5, α-$Ti(HPO_4)_2 \cdot H_2O$, can be explained in terms of the results reported in the literature (17, 18). The DTA trace corresponds to the sequence of the following processes: (i) loss of hydration water (endothermic feature at 400 K which corresponds to the formation of $Ti(HPO_4)_2$, which occurs in TGA between RT and 573 K), (ii) the α-$Ti(HPO_4)_2$ to ζ-$Ti(HPO_4)_2$ transition, a barely visible endothermic feature at 600 K), (iii) pyrophosphate formation (endothermic feature at 750 K), and (iv) phase transition of layered α-TiP_2O_7 to cubic-TiP_2O_7 at 1125 K. The weak exothermic feature appearing in 5VTiPi at ca. 500 K must involve the combustion of oxalate groups, clearly visible in the 20VTiPi trace. The peak located trace at 1125 K in α-TiP shifts to lower temperatures as vanadium loading increases (in the 20 VTiPi sample it is located at 872 K). Therefore the addition of V promotes the transformation of layered α-TiP_2O_7 to the cubic-TiP_2O_7 phase.

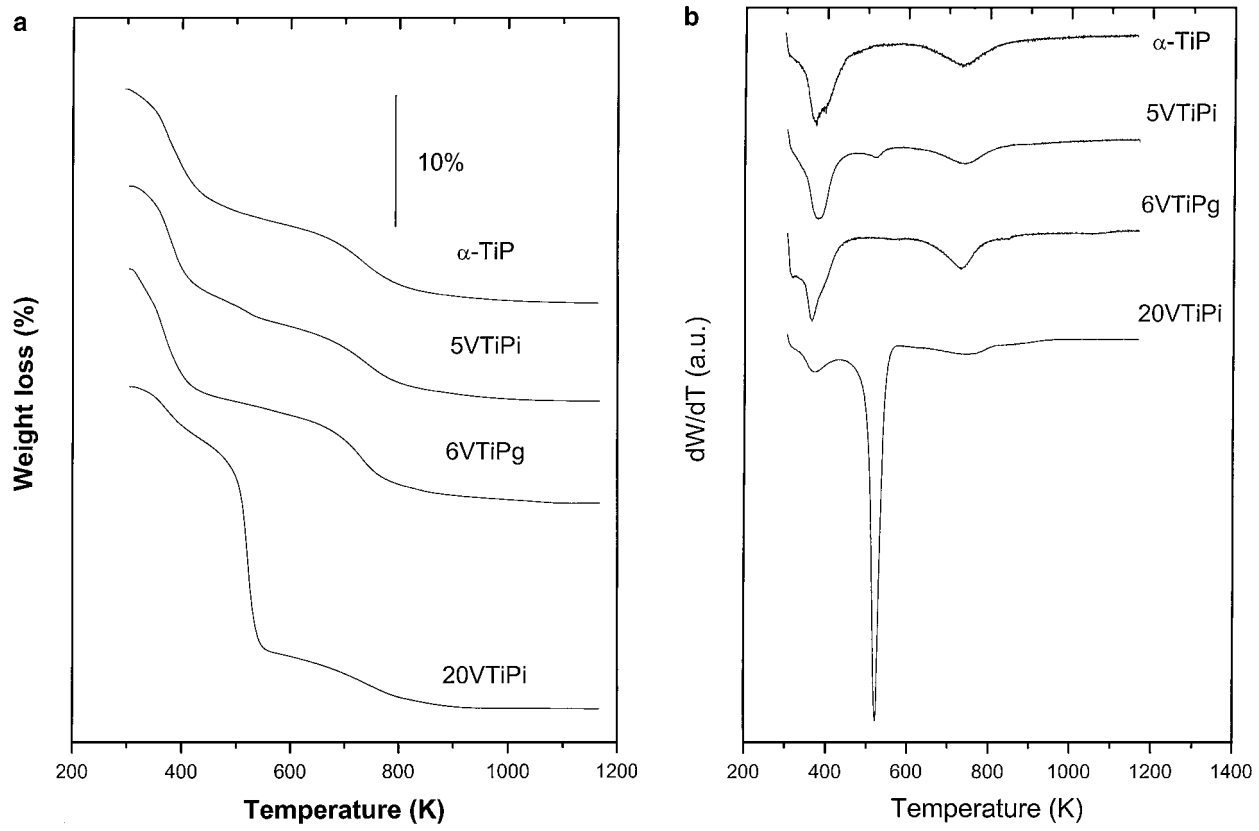

FIG. 4. (a) TG analysis of several catalysts under a flow of air. (b) Derivative curves of the former TG traces.

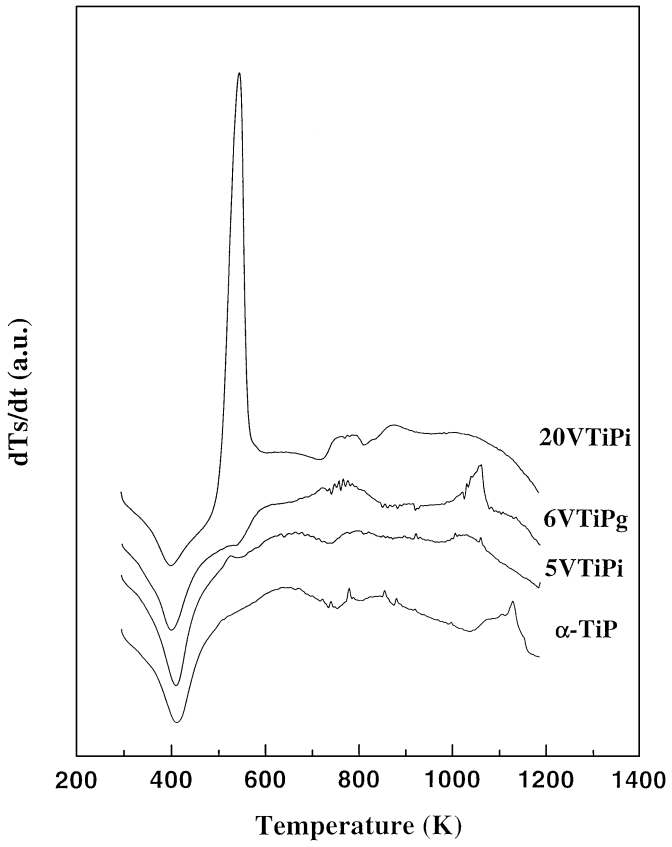

FIG. 5. DTA traces of several catalysts under a flow of air.

Raman spectra of the support α-TiP and some V-containing samples calcined at 723 K are shown in Fig. 6. Calcination was carried out *ex situ* under room air, but before the spectra were recorded the samples were recalcined in the *in situ* cell by flowing 100 mL(STP)/min of dry air and were then cooled down under the same flow to room temperature for the recording of the spectra. The Raman spectrum of α-TiP calcined at 723 K has the bands 193 (s), 250 (w), 320 (s), 412 (s), 528 (w), 569 (m), 1024 (vs), 1042 (m), 1144 (w), and 1261 (w) cm^{-1}, which can be assigned to the stretching and deformation of HPO_4^{2-} groups (18). According to TG and DTA analyses, hydrogenphosphate groups are not totally condensed at 723 K. Therefore, the Raman spectrum must represent an intermediate state in which Ti hydrogenphosphate and pyrophosphate coexist. The lack of P–O–P symmetric stretching of other metal pyrophosphates (ca. 741 cm^{-1}) (30) has also been observed in Ti phosphate calcined at 1023 K (not showed in this figure). The Raman spectra of the vanadium-containing samples can be described as the contribution of two Raman spectra, that of the support and that of other bands arising from vanadium phases. The intensity of support bands decreases as V loading rises: this effect has been attributed to the loss in efficiency of the Raman scattering process as the colour deepens with increasing the vanadium loading.

In some cases, the assignation of the new bands to any vanadium phase is not definitive, although at the end of the discussion of Raman results a general understanding of the situation can be obtained. 5VTiPi-c, 20VTiPi-c, and 6VTiPg-c are the clearest catalysts in terms of the assignation of bands to a vanadium phase. Along with bands assignable to the titanium phosphate support, 5VTiPi-c displayed the bands 168 (w), 298 (m), 457 (w), 539 (m), 579 (m), 927 (s), 949 (w), and 969 (w). These new bands correspond to α_I-$VOPO_4$. Some bands do not show the same intensity as those corresponding to the published results of the bulk phase (31), but intensity changes can be expected when α_I-$VOPO_4$ is supported. The band at 1038 (vs) cm^{-1} can be attributed to the V=O stretching vibration of a isolated tethraedral monomeric $O{=}VO_3$ (25) unit, but it coincides with a very intense band of the support (see above). The 6VTiPg-c spectrum presents the same Raman features as the 5VTiPi-c spectrum, which clearly indicates that the method of vanadium incorporation (grafting or wet impregnation) does not affect the final vanadium phase obtained in the calcined state. Five percent V_2O_5 is close to the theoretical amount needed to develop a monolayer of well-dispersed $VO_{2.5}$ units on the surface of the support (see Table 1). Therefore, it seems that vanadium precursor

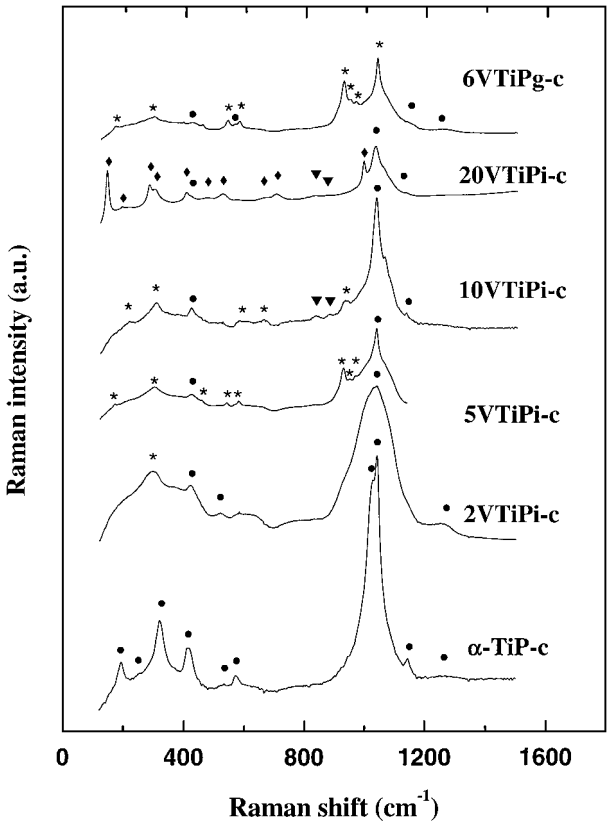

FIG. 6. Raman spectra of several catalysts (●, Ti phosphate; ∗, α_I-$VOPO_4$; ◆, V_2O_5; ▼, see text).

deposited on the surface of the support, when calcined, forms a vanadium phosphate-like phase due to the reaction with the P–OH groups remaining on the surface of Ti phosphate, and the remaining vanadium atoms form isolated $O{=}VO_3$ units anchored on other OH groups.

At the extreme end of the composition range, the richest vanadium sample (20VTiPi-c) displays Raman features clearly assignable to V_2O_5, 142 (s), 192 (w), 283 (s), 300 (sh), 404 (m), 476 (w), 525 (m), 664 (w), 702 (m), and 993 (vs) cm^{-1} (32). Since no V_2O_5 diffraction reflections were detected by XRD, small crystals must be present on the surface of the support. Raman bands at 833 (w) and 877 (w) (▼ in Fig. 6) cannot be assigned either to V_2O_5 crystallites or to any vanadium phosphate. A tentative assignment could be dimeric vanadate-type and polymeric polyvanadate-type species supported on Ti phosphate since similar frequencies have been observed for these species in V_2O_5 deposited on other supports (25, 33, 34). The band at 1038 cm^{-1}, already discussed above, can be assigned to overlapping of isolated $O{=}VO_3$ and to the support. The 10VTiPi-c sample displayed a Raman spectrum different from the former spectra. Bands at 168 (w), 298 (m), 417 (m), 579 (w), 664 (w), 833 (w), 877 (w), 931 (w), 1033 (s), 1063 (sh), and 1131 (w) are detected. The assignations of these bands are proposed in Fig. 6. This is not definitive, but it is clear that the 10VTiPi-c sample represents an intermediate state of the vanadium phase between that of the 5VTiPi-c (only α_I-$VOPO_4$ was detected) and that of 20VTiPi-c (mainly V_2O_5 is detected). The spectrum of the 2VTiPi-c catalyst shows one band not assignable to the Ti phosphate support, at 294 cm^{-1}, which can be attributed to α_I-$VOPO_4$.

Table 2 summarises some of the data obtained from XPS analysis. The XPS parameters of the 8VTi-c sample are also tabulated for comparative purposes. In the 8VTi-c catalyst, the V/Ti atomic ratio determined by XPS is much higher than the bulk value. Many authors have reported that at high vanadium loading vanadium oxide is well dispersed on the surface of the anatase as multilayers of amorphous V_2O_5 (6, 7, 35). The photoelectrons arising from the TiO_2 support are quenched by outer vanadium oxide, and the XPS V/Ti ratio is higher than in the bulk. Comparison between the XPS and bulk atomic V/Ti values in the V–Ti–P–O series shows that in all cases the XPS and bulk parameters are similar (within experimental error). This is to be expected in the samples poorest in vanadium because, at least theoretically, vanadium cannot cover the surface, and therefore the XPS signal rises from both the support and the vanadium phase. However, at the other extreme of the series, 20VTiPi-c has enough vanadium to develop several monolayers of vanadium on the surface of the support. This indicates that vanadium is not very well dispersed, forming monolayers, but rather, it forms crystallites of V_2O_5 at higher vanadium concentrations. In all cases, the XPS P/Ti atomic ratio is higher than 2 (bulk atomic ratio), which suggests that the surface is P enriched.

TABLE 2

Binding Energies (BE) of Core Electrons and Atomic Ratios of Some Catalysts (Both Sets of Values Obtained by XPS Analysis) along with the V/Ti Bulk Ratios (Determined by Chemical Analysis)

Sample	XPS V/Ti atom	XPS P/Ti atom	Bulk V/Ti atom
α-TiP-c	—	2.66	—
2VTiPi-c	0.03	2.56	0.05
5VTiPi-c	0.07	2.21	0.14
6VTiPg-c	0.13	2.74	0.14
10VTiPi-c	0.35	2.62	0.32
20VTiPi-c	0.85	2.32	0.68
8VTi-c	0.43	—	0.08

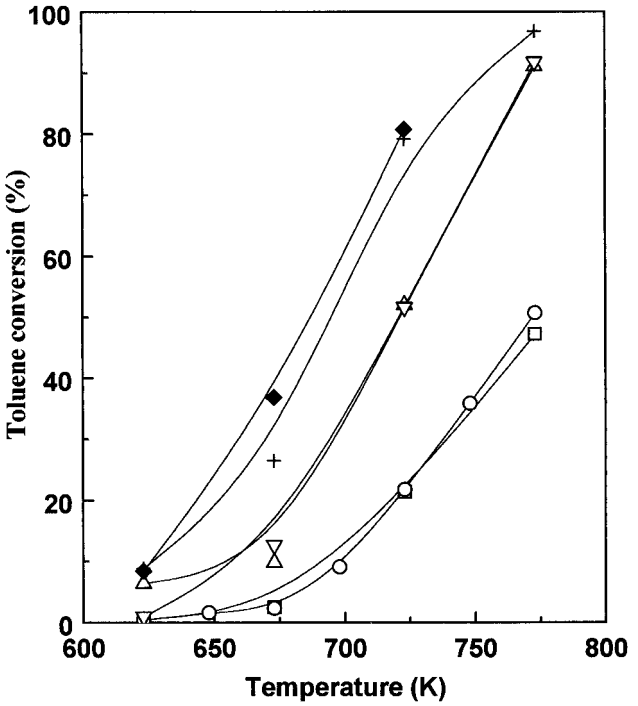

FIG. 7. Toluene conversion of several catalysts (see text for experimental conditions): □, α-TiP-c; ○, 1VTiPg-c; △, 5VTiPi-c; ▽, 6VTiPg-c; +, 20VTiPi-c; ◆, 8VTi-c.

Figure 7 shows the toluene conversion of some of the catalysts studied in this work. Table 3 shows the product yields at 723 K for the samples represented in Fig. 7 under the same feed conditions. Among the partially oxidised products detected, benzaldehyde (BCHO), benzoic acid (BCOOH), phthalic anhydride (PA), maleic anhydride (MA), and anthraquinone (ANQ) appear at the highest yields. Other minor products are *o*- and *p*-methyl-diphenyl methanone (*o*- and *p*-MDPMO), di-phenyl methanone (DPMO), and benzene (BZ). It is clearly showed that the

TABLE 3

Toluene Conversion and Yield to Main Oxidation Products at 723 K

Catalyst:	α-TiP-c	1VTiPg-c	6VTiPg-c	5VTiPi-c	10VTiPi-c	20VTiPi-c	8VTi-c
Conv (%)	21.4	21.8	51.6	52.0	80.0	79.2	80.8
Y COx (%)	13.6	15.9	29.6	24.9	33.9	29.1	40.3
Y Bz (%)	0.6	0.7	0.8	0.7	1.2	1.0	0.2
Y MA (%)	0.0	0.0	0.0	2.5	10.5	11.9	10.5
Y BCHO (%)	2.7	1.9	9.4	7.6	9.8	10.2	6.0
Y BCOOH (%)	1.6	1.9	5.4	3.4	6.3	6.0	7.5
Y PA (%)	2.4	0.9	4.8	8.3	11.6	8.7	2.1
Y ANQ (%)	0.3	0.3	1.4	4.4	6.2	4.9	1.1
Y others (%)	0.2	0.2	0.2	0.2	0.5	7.4	13.1

Note. Conditions: 0.06 g ($W/F = 42$ g s/l). Molar concentrations: toluene 0.8%, O_2 20.8%, N_2 78.4%.

incorporation of vanadium improves the catalytic performance of the bare support. When temperature was raised, toluene conversion increased and the selectivity to partial oxidation products decreased as total combustion increased. At similar toluene conversion, the richer V catalysts are more selective to partial oxidation than the V poorer samples. The carbon balance in most of the Ti phosphate supported catalysts are within the experimental error in all cases and at all temperatures. But in 20VTiPi-c and in 8VTi-c the carbon balance is 100% at lower conversion (within the experimental error) while at higher conversion it lies between 85 and 95%. The imbalance must be assigned to heavier oxidised products, such as MDPMOs, DPMO, and other even heavier products, with quite high boiling points (e.g., anthraquinone melts at 558 K), which hinders their analysis by GC. These heavy products are not totally soluble in acetone. Thus, at higher conversion and higher yields they could remain unsolubilised by the acetone. The use of other solvents such as methanol, cyclohexane, dicloromethane, butanol, acetonitrile, benzene, and octanol did not substantially improve the carbon balance. They are referred to as "other" products in Table 3 and are derived from the carbon imbalance. An important aspect is that the method of V incorporation does not seem to be so critical as regards the catalytic activity of the system. Thus, 5VTiPi-c and 6VTiPg-c catalysts, which have similar effective V loadings, have fairly similar catalytic properties. The effect of the calcination temperature, 723 K for the impregnated samples and 923 K for the grafted series, does not seem to determine the final catalytic activity.

Basically, the toluene conversion on 10VTiPi-c and 20VTiPi-c catalysts is quite similar to that of the conventional catalyst 8VTi-c. They show less theoretical amounts of V per m^2 than does 8VTi-c but show lower total oxidation levels (lower CO_x selectivity), higher BCHO and PA yields, and less heavy product formation. It can be also seen that V loadings above 10 wt% V_2O_5 do not improve the catalytic oxidation of toluene to any remarkable extent; conversions and yields to partially oxidised products remain rather unaffected. It is clear that the presence of P in the system is not detrimental in terms of conversion and results in a higher formation of PA and BCHO than that afforded by the conventional catalyst.

The relatively good catalytic properties in toluene oxidation of V–Ti–P–O catalysts as compared to a conventional catalyst, as well as the high PA selectivity, encouraged us to test *o*-xylene oxidation on these catalysts. Figures 8 and 9 and Table 4 summarise the results for the oxidation of *o*-xylene on the most selective catalysts in *o*-xylene oxidation. *o*-Xylene is transformed to partially oxidised products and, if oxidation proceeds totally, to carbon oxides. Among the partially oxidised products, *o*-tolualdehyde (*o*-TAL), phthalic anhydride (PA), and phthalide (PL) are the most important. Conventional 8VTi-c catalyst oxidizes the *o*-xylene faster than Ti phosphate supported catalysts (which was not the case in toluene oxidation). The 8VTi-c catalyst is more active and selective than the V-richer V–Ti–O–P samples. The selectivity to PA in the 8VTi-c system increases smoothly with temperature to the detriment of the

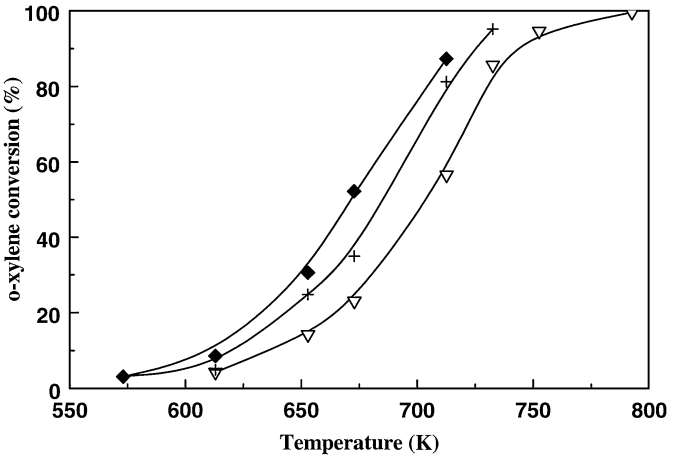

FIG. 8. *o*-Xylene conversion for most selective catalysts: ▽, 10VTiPi-c; +, 20VTiPi-c; ◆, 8VTi-c.

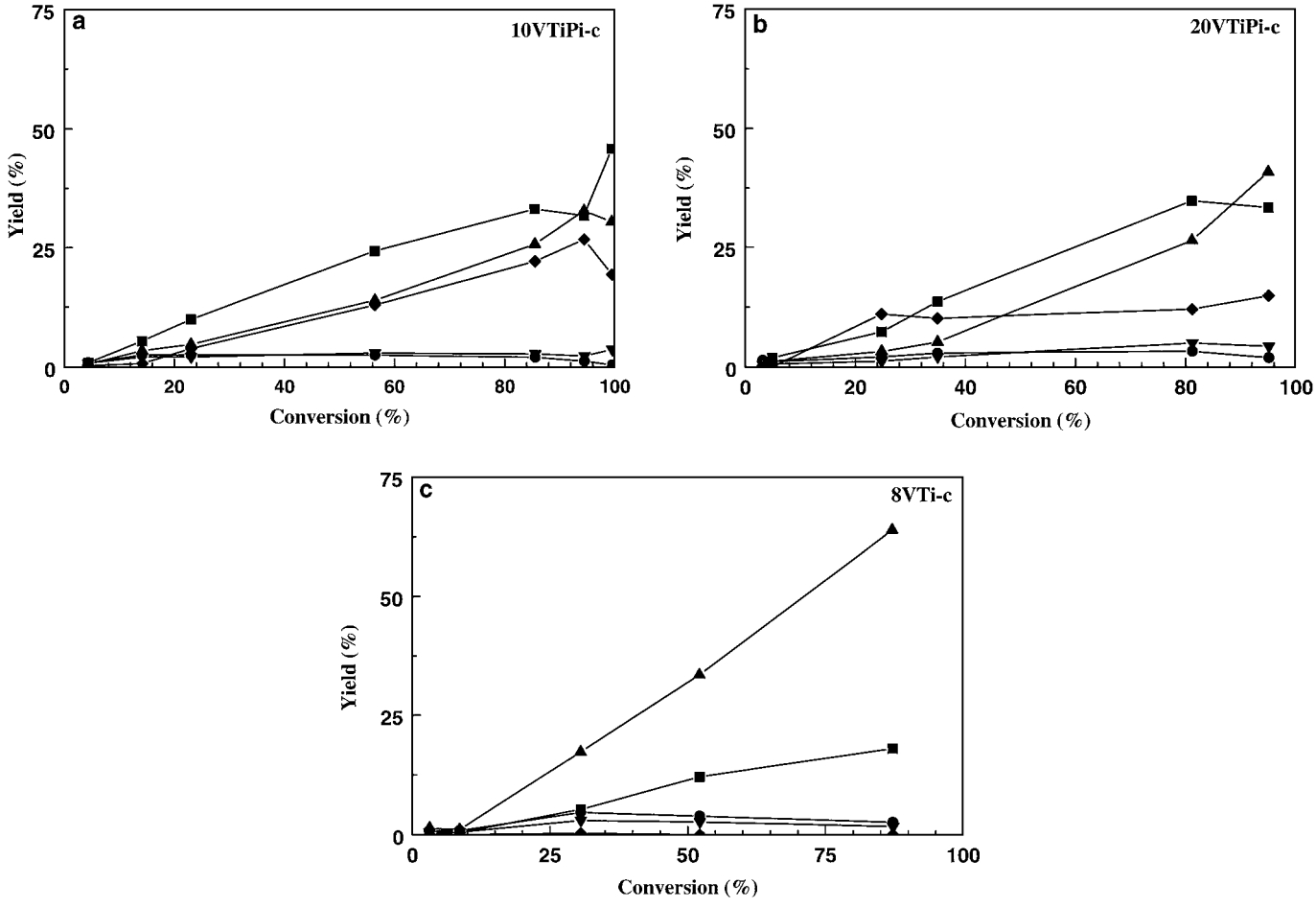

FIG. 9. Selectivities to different products of *o*-xylene oxidation: ▲, pthalic anhydride; ▼, phthalide; ●, *o*-tolualdehyde; ■, CO_x; ◆, others; (a) 10VTiPi-c; (b) 20VTiPi-c; (c) 8VTi-c.

selectivities of *o*-TAL and PL: *o*-TAL and PL are strongly oxidised to PA as conversion rises, as has also been reported in the literature (36).

The 8VTi-c catalyst is quite selective to PA, and the carbon balance is higher than 99% throughout the temperature range studied. However, in V–Ti–P–O catalyst, the CO_x yield is higher and PA formation is lower. Additonally, the loss of carbon balance is important at higher conversion (within 15–25%), indicating that there are other products which are not being analysed under these conditions. A deposit of products was observed at the bottom of the reactor (the cooler zone of the glass reactor), upstream from the condensation trap. This zone is subject to temperatures higher than 623 K, and hence the observed products must be nonvolatile and very likely result from the condensation of aromatics rings (heavy polyaromatic rings) (37–39). For two reasons, analysis of this deposit was quite difficult. One fraction was insoluble in acetone and in many other polar and nonpolar solvents. And the maximum temperature of the GC injection port rendered volatilisation of these heavy products almost impossible. In Fig. 9 carbon balance is accounted for as "other" products. In sum, Ti-phosphate-supported vanadia catalysts with V loading similar to that of a convetional V/TiO_2 catalyst are less active and less selective, and they present higher yield to heavy products.

TABLE 4

***o*-Xylene Conversion and Selectivity to Yield Oxidation Products at 713 K**

Catalyst:	10VTiPi-c	20VTiPi-c	8VTi-c
Conv (%)	56.5	81.2	87.3
Y COx (%)	24.3	34.7	19.0
Y *o*-TAL (%)	2.5	3.2	2.6
Y PA (%)	13.9	26.4	63.9
Y PL (%)	2.9	4.9	1.8
Y others (%)	12.9	12.0	0.0

Note. Conditions: 0.06 g ($W/F = 42$ g s/l). Molar concentrations: toluene 0.8%, O_2 20.8%, N_2 78.4%.

DISCUSSION

One of the first questions to be answered concerning the use of Ti-phosphate-supported vanadium oxide materials as catalysts is whether the vanadium phase is dispersed over the surface of the support, whatever the vanadium and Ti phosphate phases formed when precursors are calcined, by an interaction between the vanadium and the Ti phosphate phases that forces the vanadium phase to spread over the support phase. If not, only a physical mixture of the vanadium phase and the support will be formed, a dilution of vanadium oxide in Ti phosphate. The characterisation results can assess whether a dispersed vanadium phase is obtained. No segregation of the vanadium and titanium phases was detected by SEM, at least up to the resolution permitted by the magnification. No vanadium phase was detected in any of the catalysts by XRD, even in the 20VTiPi-c catalyst, which was the vanadium-richest sample. However, no conclusion concerning the dispersion of the vanadium phase on the support surface can be reached. One very striking observation, already commented on in Results, is that when the solid arising from the water evaporation of the impregnating solution is mixed with the support (at 20 V_2O_5 wt%) and the physical mixture is calcined at 723 K, very narrow and intense diffraction peaks of V_2O_5 are detected. All these results indicate that wet impregnation or grafting methods are needed to obtain small a crystal size in the vanadium phase. Nonetheless, a small crystal size is not itself evidence of a vanadium phase–support interaction and a more in-depth scrutiny of the results is needed.

Attention must be focused in the limited V loading reached by the grafting method. This figure (ca. 5 V_2O_5 wt%) is also close to the value at which there is a theoretical monolayer of V_2O_5 on the surface of the support, assuming that vanadum oxide is spread over the surface. Two results support the existence of a vanadium phase–support interaction at V loadings lower than one theoretical monolayer of V_2O_5. First, according to DTA analysis, transformation from layered to cubic TiP_2O_7 occurs at increasingly lower temperatures throughout the vanadium loading range, irrespective of whether the grafting or the wet impregnation method is used. This temperature shift is difficult to understand without invoking the effect of a vanadium–support interaction. If only a physical mixture of phases were present, and therefore vanadium would not affect the Ti phase through any kind of interaction, the phase change from layered to cubic would not shift to lower temperatures.

The above result is only evidence of the effect of the vanadium phase on the phase changes of Ti phosphate. The following result is a stronger indication of the existence of an interaction between the vanadium phase and the support: 5VTiPi-c and 6VTiPg-c show the same vanadium phase when calcined (as detected by Raman characterisation). Both samples have a vanadium loading close the theoretical monolayer of vanadium oxide. The fact that when the vanadium is incorporated α_I-$VOPO_4$ is formed after calcination, irrespective of the V addition method, is indication of an interaction. The interaction is defined by the reaction of VO_x moieties with Ti–OH and P–OH surface groups, which occurs directly with the grafting method. In the case of wet impregnation, a monolayer of VO_x moieties is spread over the surface of the Ti phosphate, also resulting in the formation of such bonds (evidently not during impregnation but when system is calcined).

Wet impregnation permits the vanadium loading to be increased. However, does the additional vanadium spread over the surface of such a monolayer of VO_x moieties, driven by a vanadium phase–support interaction? XPS revealed that the atomic V/Ti ratio at the surface is close to the bulk ratio throughout the V concentration range. These data suggest that the Ti XPS signal of the support is not quenched by the presence of a V phase on the surface. If successive monolayers of vanadium oxide were formed on the support the Ti signal would decrease considerably, and this is not the case. For the 8VTi-c sample, the XPS signal is much stronger than the bulk ratio: the formation of V_2O_5 crystallites on top of well-dispersed VO_x seems to be the cause of this effect (35). It can be concluded that crystals of vanadium oxide present on the surface of Ti phosphate are much larger and more poorly dispersed than on the TiO_2 support, leaving most of the support surface uncovered.

A model of the relationships between vanadium phases and the Ti phosphate support can be envisaged. When the theoretical vanadium loading approaches the amount required to cover the surface of the support, ca. 5 V_2O_5 wt%, VO_x moieties interacting with the support are present (α_I-$VOPO_4$-like environment). Since Ti–OH surface groups are available, anchored moieties on Ti sites are also expected to be present on the surface. In any case, at vanadium loadings lower than 5 wt%, a vanadium phase–support interaction exists. Upon increasing the V loading by wet impregnation, V_2O_5 microcrystals are developed in the 20VTiPi-c sample. The size of such V_2O_5 crystals is larger and they are more poorly dispersed than in the V_2O_5/TiO_2 catalyst. This means that the vanadium–Ti phosphate support interaction is weak at higher vanadium concentrations: vanadium forms vanadium oxide crystals rather than spreading over the surface. The decrease in large mesopores in the 20VTiPi-c sample suggests that such oxide crystals fill the pores defined by the clusters of the support sheets. Samples 8VTi-c and 20VTiPi-c have nearly the same number of theoretical V_2O_5 monolayers. However, the characterisation results clearly showed that V dispersion is lower on the Ti phosphate support, leaving an important fraction of the support uncovered. In contrast, several layers of amorphous vanadium oxide completely covering the TiO_2 surface are present in the 8VTi-c sample (6, 7, 35). Obviously, a larger number of vanadium sites are exposed in the conventional catalyst.

It is clear that the surface of uncovered Ti phosphate is beneficial for partial toluene oxidation, particularly for PA formation, and is unfavourable for partial *o*-xylene oxidation. It has been reported that the Ti hydrogen phosphate shows medium acid strength sites, of both Lewis and Brønsted types (40) (P–OH groups and CUS Ti sites). A conventional V–Ti–O surface also displays such acid sites, but P–OH Brønsted sites are expected to be stronger. The influence of the acid sites on the different paths of oxidation of these alkylaromatic substrates is far from understood yet. Any attempt at explanation is out of the scope of this work, which only intends to report the catalytic properties of Ti phosphate supported catalysts. But the P–OH acid sites provided by the uncovered support appear to be a key factor in explaining these differences. PA formation from toluene oxidation derives from the condensation of two toluene molecules and from *o*-xylene arising from the direct oxidation of the side chains (36). Results seem to indicate that P–OH acid sites of the Ti phosphate support facilitate the PA formation from toluene oxidation. It is hypothesised that condensation of the alkylaromatic rings demands stronger Brønsted acid sites, available in a Ti phosphate based catalyst, which supply the intermediates for a supposedly more selective PA formation route. However the same P–OH groups are detrimental for *o*-xylene oxidation and are favourable for heavy products and CO_x formation.

ACKNOWLEDGMENTS

Mrs. L. Bajón is gratefully acknowledged for her contribution in taking the SEM micrographs. The authors also appreciate Dr. M. Yates for the helpful discussion of N_2 adsorption. This work was supported by the European Commission (BRITE-EURAM programme BRPR-CT95-0062) and by the CICYT (Spain) under project MAT96-2058-CE.

REFERENCES

1. Jonson, B., Robenstorf, B., Larsson, R., and Andersson, S. L. T., *J. Chem. Soc. Faraday Trans. 1* **84**, 3547 (1988).
2. Dias, C. R., and Farinha Portela, M., *Catal. Rev. Sci. Eng.* **39**, 169 (1997).
3. Nikolov, V., Klisurski, D., and Anastasov, A., *Catal. Rev. Sci. Eng.* **33**, 319 (1991).
4. Wainwright, M. S., and Foster, N. R., *Catal. Rev. Sci. Eng.* **19**, 211 (1986).
5. Busca, G., Marchetti, L., Centi, G., and Trifirò, F., *Langmuir* **2**, 568 (1986).
6. Centi, G., *Appl. Catal.* **147**, 267 (1996).
7. Grzybowska-Swierkosz, B., *Appl. Catal.* **157**, 263 (1997).
8. Andersson, S. L. T., *J. Chem. Soc. Faraday Trans. 1* **82**, 1537 (1986).
9. Van Hengstum, A. J., Pranger, J., van Ommen, J. G., and Gellings, P. J., *Appl. Catal.* **11**, 317 (1984).
10. Deo, G., and Wachs, I. E., *J. Catal.* **146**, 335 (1994).
11. Zhu, J., Rebenstorf, B., and Andersson, S. L. T., *J. Chem. Soc. Faraday Trans. 1* **85**, 3645 (1989).
12. Soria, J., Conesa, J. C., López Granados, M., Mariscal, R., Fierro, J. L. G., García de la Banda, J. F., and Heinemann, H., *J. Catal.* **120**, 457 (1989).
13. Clearfield, A., and Thakur, D., *Appl. Catal.* **26**, 1 (1986).
14. Ramis, G., Busca, G., Lorenzelli, V., La Ginestra, A., Galli, P., and Masucci, M. A., *J. Chem. Soc. Dalton Trans.*, 881 (1998).
15. Tegehall, P. E., *Acta Chem. Scand.* **40**, 507 (1986).
16. Bruque, S., Aranda, M. A. G., Losilla, E., Olivera-Pastor, P., and Maireles-Torres, P., *Inorg. Chem.* **34**, 893 (1995).
17. Costantino, U., and La Ginestra, A., *Thermochim. Acta* **32**, 241 (1979).
18. Slade, R. C. T., Knowles, J. A., Jones, D. J., and Rozière, J., *Solid State Ionics* **96**, 9 (1997).
19. Inumaru, K., Misono, M., and Okuhara, T., *Appl. Catal. A* **149**, 133 (1997).
20. Bond, G. C., and Tahir, S. F., *Appl. Catal.* **71**, 1 (1991).
21. Bond, G. C., Zurita, J. P., Flamerz, S., Gellings, P. J., Bosch, H., van Ommen, J. G., and Kip, B. J., *Appl. Catal.* **22**, 361 (1986).
22. Centi, G., López Granados, M., Pinelli, D., and Trifirò, F., *Stud. Surf. Sci. Catal.* **67**, 1 (1991).
23. Centi, G., Giamello, E., Pinelli, D., and Trifirò, F., *J. Catal.* **130**, 220 (1991).
24. Centi, G., Pinelli, D., Trifirò, F., Ghoussoub, D., Guelton, M., and Gengembre, L., *J. Catal.* **130**, 238 (1991).
25. Deo, G., Wachs, I. E., and Haber, J., *Critic. Rev. Surf. Chem.* **4**, 141 (1994).
26. Santamaría-González, J., Martínez-Lara, M., Bañares, M. A., Martínez-Huerta, M. V., Rodríguez-Castellón, E., Fierro, J. L. G., and Jiménez-López, A., *J. Catal.* **181**, 280 (1999).
27. Alberti, G., and Marmottini, F., *J. Colloid Interface Sci.* **157**, 513 (1993).
28. Sing, K. S. W., Everett, D. H., Haul, R. A. W., Moscou, L., Pierotti, R. A., Rouquerol, J., and Simieniewska, T., *Pure Appl. Chem.* **57**, 603 (1985).
29. JCPDS File Number 38-1468.
30. Inomata, Y., Inomata, T., and Moriwaki, T., *Spectrochim. Acta* **36A**, 839 (1980).
31. Ben Abedlouahab, F., Olier, R., Guilhaume, N., Lefebvre, F., and Volta, J. C., *J. Catal.* **134**, 151 (1992).
32. Dines, T. J., Rochester, C. H., and Ward, A. M., *J. Chem. Soc. Faraday Trans.* **87**, 653 (1991).
33. Su, S. C., and Bell, A. T., *J. Phys. Chem. B* **102**, 7000 (1998).
34. Vuurman, M. A., and Wachs, I. E., *J. Phys. Chem.* **96**, 5008 (1992).
35. Védrine, J. C., *Catal. Today* **20**, 1 (1994). [And the rest of this volume]
36. Andersson, S. L. T., *J. Catal.* **9**, 138 (1986).
37. Dias, C. R., Farinha Portela, M., and Bond, G. C., *J. Catal.* **157**, 344 (1995).
38. Dias, C. R., Farinha Portela, M., and Bond, G. C., *J. Catal.* **157**, 353 (1995).
39. Dias, C. R., Farinha Portela, M., and Bond, G. C., *J. Catal.* **162**, 284 (1995).
40. Razeboom, F., Fransen, T., Mars, P., and Gellings, P. J., *Z. Anorg. Allg. Chem.* **449**, 25 (1979).